

Field emission of individual carbon nanotube with *in situ* image and real work function

Zhi Xu, X. D. Bai, and E. G. Wang^{a)}

International Center for Quantum Structures, Institute of Physics, Chinese Academy of Sciences, Beijing 100080, China

Zhong L. Wang

School of Materials Science and Engineering, Georgia Institute of Technology, Atlanta, Georgia 30332-0245

(Received 4 January 2005; accepted 22 August 2005; published online 10 October 2005)

The field emission properties of individual multiwalled carbon nanotubes have been measured simultaneously in correlation to the emitter images and their real work functions at tips by the *in situ* transmission electron microscopy method. The field emission of a single nanotube still follows the Fowler-Nordheim law. The field enhancement factor has been determined by the real work function rather than a given constant. *In situ* imaging and measurement show that the work function at the nanotube tip depends strongly on its structure and surface condition. This study provides an approach of direct linking field emission with the *in situ* emitter structure and the real work function at the emitter tip. © 2005 American Institute of Physics. [DOI: 10.1063/1.2103420]

Field emission is one of the most promising applications of carbon nanotubes (CNTs) for flat panel displays¹ and highly coherent field-emission electron gun in an electron microscope.² Field emission of nanotubes have many excellent properties such as low turn-on fields and high emission currents,^{3,4} stable emission current,^{5,6} long life time,^{7,8} low energy spread,⁸ and high brightness.² Most of the previous studies have been focused on the statistical properties of a large number of collective nanotubes. Because the structure of an individual nanotube strongly affects its field emission properties, the field emission of individual nanotubes began to attract considerable attention. The study on individual CNTs inside scanning electron microscopy⁹ (SEM) suggested that only a very small proportion of exceptional long and/or narrow nanotubes with higher field enhancement factors contribute to the emitted current in usual large area measurements. Recently, structure damage during field emission was directly imaged by *in situ* transmission electron microscopy (TEM).^{10,11} In the meantime, some theoretical calculations have been carried out to study the dependence of field-emission characteristics of CNTs on their electronic and structural properties.^{12–17} However, almost all of the previous studies on carbon nanotube field emission took the work function as a constant (e.g., 5 eV). Actually, the surface condition of an emitter strongly affects its work function, and the surface condition varies greatly among different nanotubes. Thus, it is important to measure the real work function at the nanotube tip simultaneously during the field emission.

In this letter, we present an *in situ* TEM measurement, which directly links the field emission properties of a single nanotube with its structure and the real work function at the nanotube tip. The field emission of a single nanotube still follows the Fowler-Nordheim (F-N) equation, and the field enhancement factor has been determined by the real work function measured *in situ*. It was found that the work function at the nanotube tip depends strongly on its structure and

surface condition. This study first makes the field emission to be correlated with the real work function of the emitting nanotube, and the structure of the nanotube can be imaged at the same time.

For *in situ* observation and measurement, a special TEM specimen holder was built for a JEOL 2010 FEG TEM operated under the vacuum of 10^{-7} Torr and at room temperature. The schematic frame is shown in Fig. 1(a). An electrochemically etched tungsten needle served as the movable cathode, its opposite gold panel was the anode. The distance between two electrodes can be adjusted from several hundreds to several tens of nanometers. The multiwalled CNTs

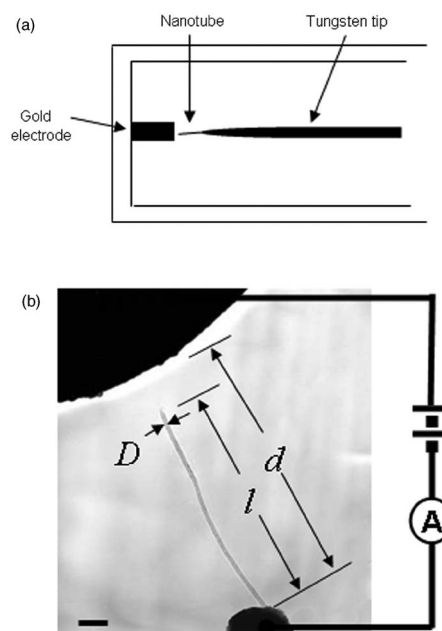


FIG. 1. (a) Schematic drawing of the homemade TEM specimen holder for *in situ* measurements. (b) Typical experimental configuration and definition of geometrical parameters. Another dc power supply will be applied together with the ac power when measuring the local work function at emitter tip. Scale bar: 200 nm.

^{a)} Author to whom correspondence should be addressed; electronic mail: egwang@aphy.iphy.ac.cn

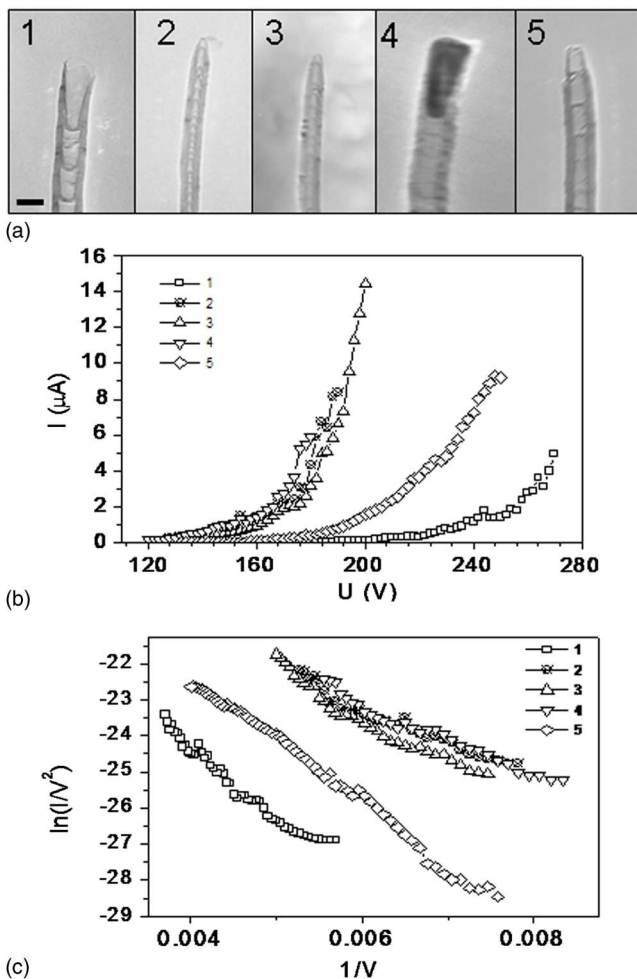


FIG. 2. (a) TEM images of emitting tips for nanotubes 1–5. Nanotubes 2 and 3 is the same tube but nanotube 2 has amorphous carbon adhered on it. After several electric field scanning cycles, the amorphous carbon was burned out (nanotube 3). Scale bar: 50 nm. (b) I - V curves of different nanotubes marked by 1–5 in Fig. 2(a). (c) Corresponding F-N plots.

were grown by the microwave plasma enhanced chemical vapor deposition method.^{5,18} An individual nanotube is mounted on the tungsten needle by a piezodriven nanomanipulator equipped in a SEM. The needle with the stuck nanotube is fixed on the specimen holder to carry out the field emission and work function measurements. An example of individually mounted CNT is given in Fig. 1(b), in which the electric circuit and the specific size, i.e., the interelectrode distance d , the length l , and diameter D of the CNT, for field emission measurements are shown. Because of the small interelectrode distance, the turn-on voltage is as low as 100 V, compared to that of >1000 V in the case of carbon nanotube film emission. Another alternating signal power is applied together with the dc power to measure the work function at the tip of a nanotube following the method developed by Gao *et al.*¹⁹ During TEM characterization, care has been taken to minimize contamination effect and to blank out the electron beam during I - V and work function measurements.

The free standing CNTs were imaged in the TEM, which exhibit different tip structures: open end, closed end with contamination, closed end with clean surface, with catalyst particle on top, and those with peeled off caps, as indicated by numbers 1–5 in Fig. 2(a), respectively. Their I - V curves and corresponding F-N plots are shown in Figs. 2(b) and

2(c). The emission current increases exponentially while increasing interelectrode voltage. Their turn-on voltage is different due to the different interelectrode distance and the different field enhancement factor²⁰ for the five cases presented earlier. A single nanotube with diameter of 31.7 nm [number 2 in Fig. 2(a)] can endure a current of 14.5 μA , and after some time the top surface became clean. But its turn-on field increased, which suggests that the field emission performance may be improved by the contamination and/or adsorbate on the emitter tip, although the performance is unstable.

The F-N plot [$\ln(I/V^2)$ vs $1/V$, where I is emission current and V is applied voltage] [see Fig. 2(c)] can be approximately fitted to a straight line, in agreement to the expected result from the Fowler-Nordheim equation, which correlates the emission current with the surface potential, in agreement with that of the others.^{9,21} In the F-N theory, the field emission current is determined by two factors: field enhancement factor β and work function ϕ , which is expressed as

$$I = KF^2/\phi \exp(-B\phi^{3/2}/F), \quad (1)$$

where $B = 6.83 \times 10^9 \text{ V eV}^{-3/2} \text{ m}^{-1}$, K is a constant. The local electric field F is usually related to the applied voltage V as $F = \beta V/d$, where β quantifies the ability of amplifying the average field V/d , it is named as the field enhancement factor. The conventional way to determine β from the measurements is to trace a F-N plot, whose slope k can be expressed as

$$k = -B\phi^{3/2}d/\beta. \quad (2)$$

According to Eq. (2), if the work function is known, the field enhancement factor β can be deduced from the slope k of the F-N plot.

In previous research, since it is difficult to measure the actual local work function of the emitter, the work function of graphite is usually taken as that of carbon nanotubes. In fact, the work function is very sensitive to the atomic structure and the surface condition of the emitting tip, thus it certainly deviates from the work function of graphite. For example, in the cases of nanotubes 2 and 3, as shown in Fig. 2, although they have the same tube geometry, a large difference of field emission behavior has been demonstrated. At the beginning, there was some amorphous carbon sticking at the tip. After several cycles of measurements, the amorphous carbon was burnt out by the emission current, and only a clean tube cap left. The field emission properties are quite different between the two cases.

In this study, we measured the work function at the tip of individual nanotube by *in situ* TEM. The nanotube was first excited to the mechanical resonance state by applying an alternating electrical field across the two electrodes.²² Then a direct current voltage V_{dc} is added to the alternative voltage. Based on the principle of contact potential difference, if the work function of the gold electrode is ϕ_{Au} , the work function of the nanotube tip ϕ_T is determined by the V_{dc} at which the vibration amplitude of the nanotube is zero.¹⁹ Figure 3 shows an example before and after the amplitude of a resonance nanotube was brought to zero by adjusting V_{dc} (see the details in Refs. 19 and 23).

The systematical data are summarized in Table I, in which the geometry parameters l , d , and D defined in Fig. 1(b), the fitted slope k of the F-N curve in Fig. 2(b) (symboled $k_{\text{F-N}}$), work function ϕ , the real field enhancement factor β , and the calculated field enhancement factor by taking

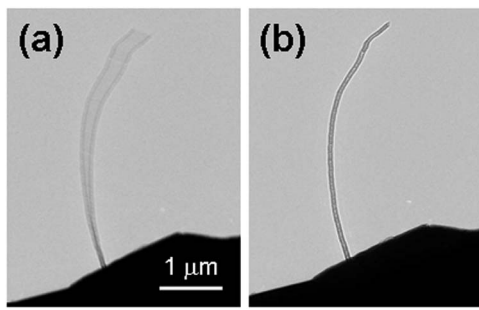


FIG. 3. Measurement of local work function. (a) Natural resonant state of an individual nanotube at tungsten tip. Scale bar: 500 nm. (b) When an appropriate dc voltage is applied across the nanotube and its counterpart electrode, the amplitude of vibration is adjusted to zero. In this case, $V_{dc} = -0.32$ V, $\phi_r = 4.78$ eV.

work function as a constant of 5 eV (symboled β') are listed for the five cases presented in Fig. 2, respectively. It is noted that the real work functions of different nanotube structures are different. When the amorphous carbon at the tip of nanotube 2 was burned out, the work function increased significantly (for nanotube 3). This is the reason why emission performance of nanotube 3 decreases. Because the catalyst particle is covered by carbon layers in nanotube 4, the work function is close to carbon, but the effect of the iron particle on work function still exists. Also, the work functions between the open-ended and closed-ended nanotubes are different. Even both are closed-ended but their morphologies are different, such as nanotubes 3 and 5, still demonstrate different field emission behaviors. In addition, the real field enhancement factors β are quite different from the calculated β' by using a constant work function in Eq. (2). For example of sample No. 4, the difference between the two cases reaches up to 14%. It clearly shows that a constant work function ϕ used in previous studies is not good enough.

The field emission property is determined by two physical parameters: field enhancement factor and work function. They are related with several factors, such as the geometry of the nanotube, the electrode shape, the interelectrode distance, the emitter structure, and its surface conditions. So far, it is hard to exactly get the field emission information corresponding to every factor. In the present study, our main purpose is to determine these factors directly from the *in situ* TEM images obtained during emission. Since the work function of an emitter can be measured by *in situ* TEM in this

TABLE I. Systematic field emission data of for the five typical samples.

Sample No.	$l/\mu\text{m}$	$d/\mu\text{m}$	D/nm	k_{F-N}	ϕ/eV	β	β'
1	0.32	2.16	52.4	-1817	4.60	80	91
2	3.9	4.3	31.7	-989	4.51	300	332
3	3.9	4.3	31.7	-1266	4.78	230	259
4	11.2	16.9	61.1	-974	4.58	1162	1325
5	6.4	8.2	46.4	-1735	4.60	319	361

setup, our field enhancement factor is obtained by the real work function rather than a given constant. This is a key step towards quantifying the field emission properties of a nanoobject with well-defined structure.

In conclusion, we have performed *in situ* measurements on the field electron emission properties and work functions of individual carbon nanotube emitters. The nanotube structure and measurement geometry can be simultaneously imaged *in situ* TEM. The field emission behavior still follows the F-N equation. It was found that the nanotube tip structure and surface condition significantly affect the local work function. Thus, the field enhancement factors are determined by the real work function at the emitting tip. A simultaneous determination of the structure and real work function while measuring the field emission behavior yield useful insights about the field emission characteristics of one-dimensional nanostructures.

This research is financially supported by the NSF (Grant Nos. 10304024 and 50472074), MOST and CAS of China. The authors acknowledge gratefully Professor C. Z. Gu for his help on the SEM experiment, and Dr. C. Y. Zhi and Dr. G. Y. Zhang for their useful discussions.

- ¹W. B. Choi, D. S. Chung, J. H. Kang, H. Y. Kim, Y. W. Jin, I. T. Tan, Y. H. Lee, J. E. Jung, N. S. Lee, G. S. Park, and J. M. Kim, *Appl. Phys. Lett.* **75**, 3129 (1999).
- ²N. de Jonge, Y. Lamy, K. Schoots, and T. H. Oosterkamp, *Nature (London)* **420**, 393 (2002).
- ³J.-M. Bonard, J. P. Salvetat, T. Stockli, L. Forro, and A. Chatelain, *Appl. Phys. A: Mater. Sci. Process.* **69**, 245 (1999).
- ⁴W. A. de Heer, A. Chatelain, and D. Ugarte, *Science* **270**, 1179 (1995).
- ⁵X. C. Ma, E. G. Wang, W. Z. Zhou, D. A. Jefferson, J. Chen, S. Z. Deng, N. S. Xu, and J. Yuan, *Appl. Phys. Lett.* **75**, 3105 (1999).
- ⁶S. T. Purcell, P. Vincent, C. Journet, and V. T. Binh, *Phys. Rev. Lett.* **88**, 105502 (2002).
- ⁷K. A. Dean and B. R. Chalamala, *Appl. Phys. Lett.* **75**, 3017 (1999).
- ⁸M. J. Fransen, T. van Rooy, and P. Kruit, *Appl. Surf. Sci.* **146**, 312 (1999).
- ⁹J.-M. Bonard, K. A. Dean, B. F. Coll, and C. Klinke, *Phys. Rev. Lett.* **89**, 197602 (2002).
- ¹⁰Z. L. Wang, R. P. Gao, W. A. de Heer, and P. Poncharal, *Appl. Phys. Lett.* **80**, 856 (2002).
- ¹¹Z. L. Wang, P. Poncharal, and W. A. de Heer, *Microsc. Microanal.* **6**, 224 (2000).
- ¹²X. Zheng, G. H. Chen, Z. Li, S. Z. Deng, and N. Xu, *Phys. Rev. Lett.* **92**, 106803 (2004).
- ¹³S.-D. Liang, N. Y. Huang, S. Z. Deng, and N. S. Xu, *Appl. Phys. Lett.* **85**, 813 (2004).
- ¹⁴G. Zhou, W. Duan, and B. Gu, *Phys. Rev. Lett.* **87**, 095504 (2001).
- ¹⁵J. Luo, L.-M. Peng, Z. Q. Xue, and J. L. Wu, *Phys. Rev. B* **66**, 155407 (2002).
- ¹⁶D. L. Carroll, P. Redlich, P. M. Ajayan, J. C. Charlier, X. Blase, A. De Vita, and R. Car, *Phys. Rev. Lett.* **78**, 2811 (1997).
- ¹⁷A. Buldum and J. P. Lu, *Phys. Rev. Lett.* **91**, 236801 (2003).
- ¹⁸Z. Xu, X. D. Bai, E. G. Wang, and Z. L. Wang (unpublished).
- ¹⁹R. Gao, Z. Pan, and Z. L. Wang, *Appl. Phys. Lett.* **78**, 1757 (2001).
- ²⁰C. J. Edgecombe and U. Valdre, *Philos. Mag. B* **82**, 987 (2002).
- ²¹N. de Jonge, M. Allieux, M. Doytcheva, M. Kaiser, K. B. K. Teo, R. G. Lacerda, and W. I. Milne, *Appl. Phys. Lett.* **85**, 1607 (2004).
- ²²P. Poncharal, Z. L. Wang, D. Ugarte, and W. A. de Heer, *Science* **283**, 1513 (1999).
- ²³X. D. Bai, E. G. Wang, P. X. Gao, and Z. L. Wang, *Nano Lett.* **3**, 1147 (2003).